

AD-A132966

TECHNICAL  
LIBRARY

AD-A132 966

TECHNICAL REPORT ARBRL-TR-02516

STANDARDIZATION OF A DROP WEIGHT  
MECHANICAL PROPERTIES TESTER FOR  
GUN PROPELLANTS

Robert J. Lieb  
Joseph J. Rocchio

July 1983



US ARMY ARMAMENT RESEARCH AND DEVELOPMENT COMMAND  
BALLISTIC RESEARCH LABORATORY  
ABERDEEN PROVING GROUND, MARYLAND

Approved for public release; distribution unlimited.

DTIC QUALITY INSPECTED 3

19970910 020

Destroy this report when it is no longer needed.  
Do not return it to the originator.

Additional copies of this report may be obtained  
from the National Technical Information Service,  
U. S. Department of Commerce, Springfield, Virginia  
22161.

The findings in this report are not to be construed as  
an official Department of the Army position, unless  
so designated by other authorized documents.

*The use of trade names or manufacturers' names in this report  
does not constitute indorsement of any commercial product.*

UNCLASSIFIED

SECURITY CLASSIFICATION OF THIS PAGE (When Data Entered)

REPORT DOCUMENTATION PAGE		READ INSTRUCTIONS BEFORE COMPLETING FORM
1. REPORT NUMBER TECHNICAL REPORT ARBRL-TR-02516	2. GOVT ACCESSION NO.	3. RECIPIENT'S CATALOG NUMBER
4. TITLE (and Subtitle) STANDARDIZATION OF A DROP WEIGHT MECHANICAL PROPERTIES TESTER FOR GUN PROPELLANTS		5. TYPE OF REPORT & PERIOD COVERED October 81 - April 82
7. AUTHOR(s) Robert J. Lieb Joseph J. Rocchio		6. PERFORMING ORG. REPORT NUMBER
9. PERFORMING ORGANIZATION NAME AND ADDRESS US Army Ballistic Research Laboratory ATTN: DRDAR-BLI Aberdeen Proving Ground, MD 21005		8. CONTRACT OR GRANT NUMBER(s)
11. CONTROLLING OFFICE NAME AND ADDRESS US Army Armament Research and Development Command US Army Ballistic Research Laboratory(DRDAR-BLA-S) Aberdeen Proving Ground, MD 21005		10. PROGRAM ELEMENT, PROJECT, TASK AREA & WORK UNIT NUMBERS 1L161102AH43
14. MONITORING AGENCY NAME & ADDRESS (if different from Controlling Office)		12. REPORT DATE Jul 83
		13. NUMBER OF PAGES 43
		15. SECURITY CLASS. (of this report) UNCLASSIFIED
16. DISTRIBUTION STATEMENT (of this Report) Approved for public release; distribution unlimited		15a. DECLASSIFICATION/DOWNGRADING SCHEDULE
17. DISTRIBUTION STATEMENT (of the abstract entered in Block 20, if different from Report)		
18. SUPPLEMENTARY NOTES Presented at the JANNAF 18th Structure and Mechanical Behavior Subcommittee Meeting, 1-3 December 1980.		
19. KEY WORDS (Continue on reverse side if necessary and identify by block number) Interior Ballistics                      Gun Propellants Mechanical Properties High Strain Rate Testing		
20. ABSTRACT (Continue on reverse side if necessary and identify by block number) mb A drop weight impact mechanical properties tester for propellant grains has been developed. The high strain rate device has been standardized with a 7075-T6 aluminum which has a strain rate independent modulus and has been found to give repeatable accurate results. The device is simple to operate and provides direct, simultaneous force and displacement measurements. Results indicate that the device will provide accurate data for high rate compressional testing of gun propellant grains.		

# TABLE OF CONTENTS

	Page
LIST OF ILLUSTRATIONS.....	5
I. INTRODUCTION.....	7
II. EXPERIMENTAL METHOD.....	8
A. The Apparatus.....	8
B. The Procedure.....	13
C. The Effect of the Rig Motion on Sample Displacement....	16
D. The Test for Noncoaxial Impact (Bending).....	18
III. RESULTS AND DISCUSSION.....	20
A. The Rig Motion.....	20
B. The DWMPT Standardization.....	20
C. The Test for Noncoaxial Impact (Bending).....	28
IV. CONCLUSIONS.....	31
V. ACKNOWLEDGEMENTS.....	31
REFERENCES.....	33
DISTRIBUTION LIST.....	35

## LIST OF ILLUSTRATIONS

Figure	Page
1. The Drop Weight Mechanical Properties Tester (DWMPT)...	9
2. Detail of the DWMPT Showing the Relationship Between the Ram, Sample, and Force Gage.....	10
3. Detail of the DWMPT Showing the Guide and Guide Support.....	11
4. Schematic Diagram of the Data Acquisition During Standardization.....	14
5. Schematic Diagram of the Data Acquisition During Normal Testing.....	15
6. Sample Showing the Location of the Strain Patches.....	17
7. Force Versus Displacement Recorded with No Sample Present in the DWMPT.....	19
8. Force and Displacement Versus Time Recorded with No Sample Present in the DWMPT.....	21
9. Stress and Strain Versus Time for 7075-T6 Aluminum....	22
10. Stress and Strain Versus Time for the Event Shown in Figure 9 Using the Strain Gage Generated Data.....	23
11. Stress and Strain Versus Time for the Event Shown in Figure 9 Using the Optical Displacement Follower Generated Data.....	24
12. Stress Versus Strain for the Curves Shown in Figure 10	25
13. Stress Versus Strain for the Curves Shown in Figure 11	26
14. Strain from Strain Gages #1 and #2 Versus Time Recorded During the Bending Test.....	29
15. Percent Difference in Strain Recorded from Gages #1 and #2 Versus Time.....	30
16. Percent Difference in Strain Versus Sample Orientation Determining the Degree of Bending Due to the DWMPT....	32

## I. INTRODUCTION

Fracture mechanics of gun propellants has become recognized as an important area of research in the gun propulsion community.<sup>1-9</sup> The ballistic performances of conventional and experimental propellants have been shown to depend on the mechanical response of the grains to the high stress and high strain rate environment experienced during the interior ballistic cycle. In interior ballistic codes, the grain is considered to be an incompressible, nondeformable solid that burns with a mass generation rate that is determined by the linear burning rate and exposed surface area. If grain fracture occurs, more surface area is exposed which results in a higher mass generation rate than planned. This leads to poor performance and possibly to gun failure. Vulnerability of a propellant is also influenced by its mechanical

---

<sup>1</sup>H. Schubert and D. Schmitt, "Embrittlement of Gun Powder," Proceedings of the International Symposium on Gun Propellants, Dover, NJ, p. 2.11, October 1973.

<sup>2</sup>P. J. Greidanus, "Simple Determination of the Mechanical Behavior of Double-Based Rocket Propellants Under High Loading Rates," Propulsion and Energetics Panel, AGARD, 47th (A) Meeting, Paper No. 23, Porz-Wahn, Germany, May 1976.

<sup>3</sup>P. Benhaim, J. L. Paulin, B. Zeller, "Investigation on Gun Propellant Break-Up and Its Effect in Interior Ballistics," Proceedings of the 4th International Symposium on Ballistics, Monterey, CA, October 1978.

<sup>4</sup>R. A. Wires, J. P. Pfau, J. J. Rocchio, "The Effect of High Rates of Applied Force and Temperature on the Mechanical Properties of Gun Propellants," 1979 JANNAF Propulsion Meeting, Vol. 1, CPIA Publication 300, pp 25-50, March 1979.

<sup>5</sup>C. W. Fong, "Mechanical Properties of Gun Propellants - An Assessment of Possible Approaches to Laboratory Testing," Report No. WSRL-0120-TM, Weapons Systems Research Laboratory, Adelaide, South Australia, December 1979.

<sup>6</sup>C. W. Fong, "Dynamic Mechanical Properties of Gun Propellants - The Relationship between Impact Fracture Properties and Secondary Loss Transitions," Report No. WSRL-0204-TR, Weapons Systems Research Laboratory, Adelaide, South Australia, March 1981.

<sup>7</sup>A. W. Horst, "The Role of Propellant Mechanical Properties in Propelling Charge Phenomenology," 1981 JANNAF Structures and Mechanical Behavior Subcommittee Meeting, Vol. 1, CPIA Publication 351, pp 141-154, December 1981.

<sup>8</sup>R. J. Lieb, J. J. Rocchio, and A. A. Koszoru, "Impact Mechanical Properties Tester for Gun Propellants," 1981 JANNAF Structures and Mechanical Behavior Subcommittee Meeting, Vol.1, CPIA Publication 351, pp 155-173, December 1981.

<sup>9</sup>C. W. Fong and B. K. Moy, "Ballistic Criteria for Propellant Grain Fracture In the GAU-8/A 30MM Gun, Report not yet published, Direct Fire Weapons Division, Air Force Armament Laboratory, Eglin AFB, FL, December 1981.



properties. It has been shown that a grain that is brittle and fractures upon exposure to a shaped charge jet or spall threat reacts more violently than a tougher, less brittle grain. Understanding the mechanical response of grains to conditions similar to those experienced during the ballistic cycle can help direct changes in the formulation or the processing techniques so the performance and vulnerability properties of the propellant can be improved.

Efforts by several groups to construct a high strain rate device have met with various degrees of success. However, the experimental apparatus used in these tests either had too low a strain rate to simulate the rates expected during the interior ballistic cycle, or the sample displacement was either calculated or inferred. To remedy this condition, a high strain rate tester that simultaneously measures sample displacement and impact force in a simple and direct manner was constructed.

The Drop Weight Mechanical Properties Tester (DWMPT) developed and tested in this study is a modified version of the drop weight tester used by Wires.<sup>4</sup> Wires developed this tester by incorporating the simultaneous measurement of force and sample displacement into a device similar to one used by Greidanus.<sup>2</sup> A standard drop weight tester was modified by Greidanus so that large pressure impulses of the magnitude experienced in rocket motors could be applied to propellant. The displacement, however, was calculated rather than being measured directly. The pressure pulses were generated by dropping a weight cage through a preselected distance onto the sample. Wires had the weight strike the sample which was mounted on a platform especially designed and equipped with strain gages to act as a load cell. The force, including its time variation, on the sample could be determined from the recorded axial strain of the platform. The displacement measurement was accomplished by optically tracking a light/dark demarcation line on a cap placed on top of the grain. Wires found that high strain rate mechanical measurements on propellants could be made consistently. The accuracy of the device was not established and may have been poor since it deduced incorrect mechanical properties for one well-documented and understood engineering material. The measured values of displacement and force, while shown to be accurate under static calibration conditions, were indirect measurements that did not take into account dynamic effects of the apparatus. Indications of eccentric impacts causing couples to act on the sample were also found.

The objectives of this study, therefore, were to develop the drop weight tester by modifying the apparatus used by Wires so that force and displacement are measured more directly, and to standardize the impact device with a material of known properties to ensure the accuracy of the measurements.

## II. EXPERIMENTAL METHOD

### A. The Apparatus

The drop weight tester developed in this study is a modified version of the tester used by Wires, described in the Introduction. The DWMPT, illustrated in Figure 1, delivers an impulse to a sample placed between the impact force transducer, attached to the base, and a specially built ram and guide, illustrated in Figures 2 and 3. The ram serves to transmit the impact

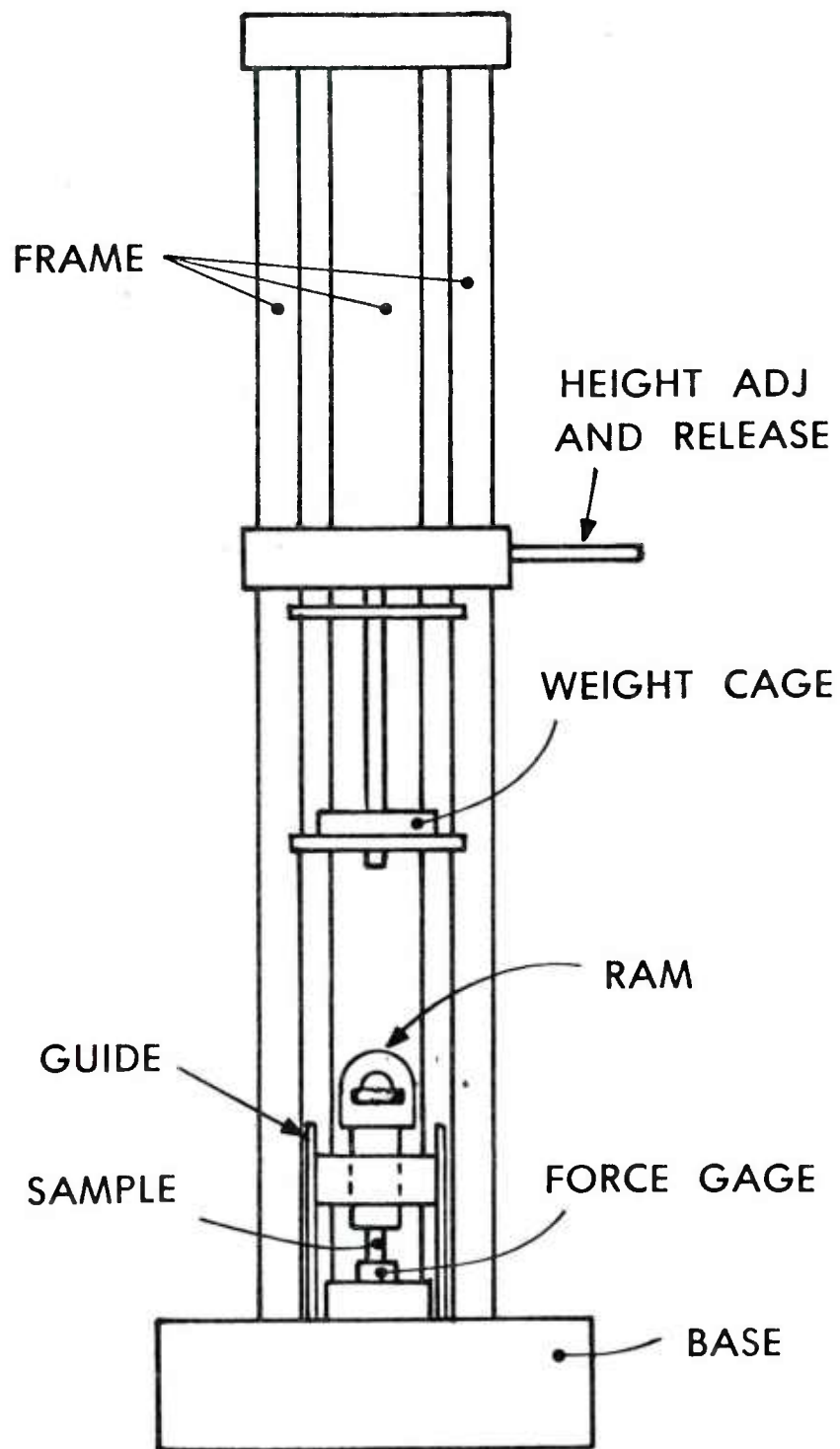


Figure 1. The Drop Weight Mechanical Properties Tester (DWMPT).



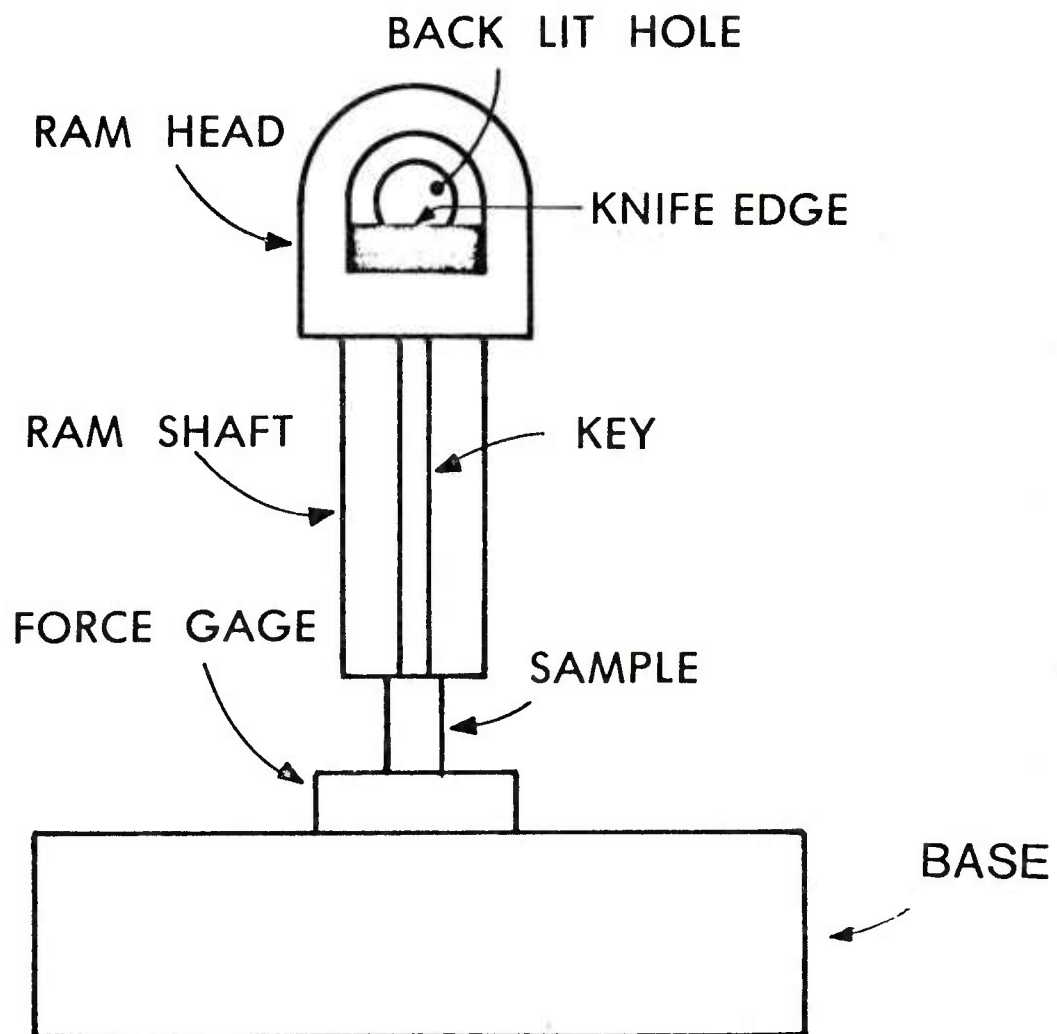


Figure 2. Detail of the DWMPPT Showing the Relationship Between the Ram, Sample, and Force Gage.

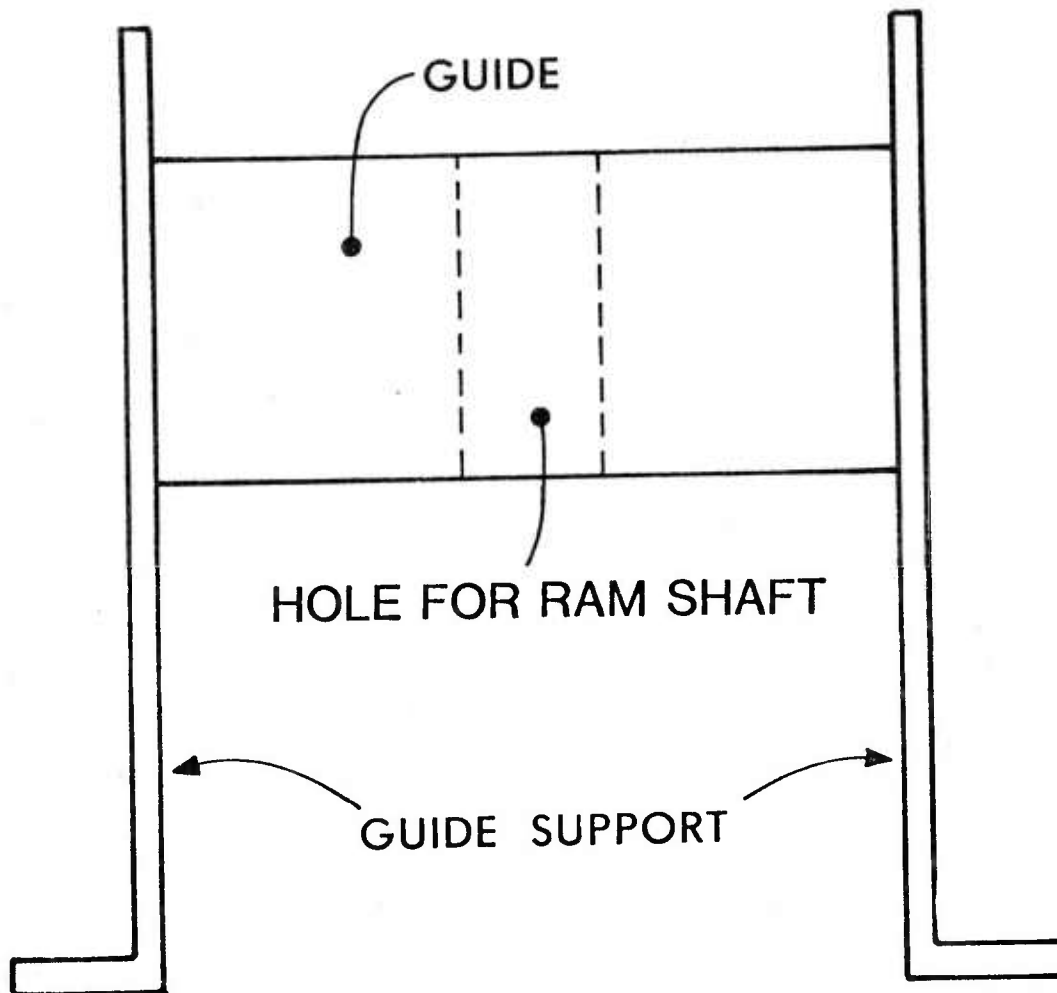


Figure 3. Detail of the DWMPPT Showing the Guide and Guide Support.

force as well as aid in the measurement of sample compression. The guide controls the ram motion so the direction of impact and sample displacement are known. The impact force is delivered by a falling weight cage for which both the mass and drop height can be adjusted. This operation is discussed in more detail below.

The DWMPT is able to record simultaneous measurements of force and displacement at ram speeds of up to 5 m/sec. A maximum force of 22 kN can be applied to a sample with a maximum diameter and length of 12.5 mm and 60 mm, respectively (although the maximum desired length would be about 30 mm to prevent sample bending). This enables gun propellant grains to be subjected to pressure impulses of up to 200 MPa, well beyond the yield strength of any grain yet tested. The smallest resolution of sample displacement in a typical drop is about 0.01 mm.

The apparatus consists of an Olin-Mathieson Drop Weight Tester, Model 7, that has been modified by putting a PCB, Model 200A, Piezotronic impact force transducer in place of the standard sample anvil. The ram and guide are mounted directly over the force transducer to record the change in length of the sample, which is placed between the ram and transducer. A 1-kg weight cage provides the impact force by falling through a preselected height (0 to 45 cm) onto the ram head. The mass of the cage can be changed (1 to 7 kg) by adding weights so the energy and velocity of impact can be varied independently.

The impact force is transmitted through the ram which is designed to aid in the measurement of change in sample length by providing a light/dark demarcation line that is tracked by an Optron Electro-Optical Displacement Follower (EODF), Model 501. Back lighting for a knife edge is provided by the illumination of a diffusion plate with an incandescent bulb supplied with a regulated DC current. The displacement follower tracks the back-lit knife edge mounted on the ram head by locking onto the demarcation line being projected onto a photoelectric screen. Electrons emitted from the screen are deflected through an aperture by magnetic coils placed along the flight path of the electrons. The current in the coils is adjusted to maximize the flow of electrons into the aperture. As the demarcation line moves, the change in the coil deflection current is measured and correlated to the distance the line moved. This method of measurement is light intensity independent, in principle, and thereby permits optical displacement measurements independent of intensity variations of the optical field.

Calibration of the displacement follower is easily made by placing feeler gages or blocks of known thickness between the force transducer and ram shaft. The voltage output can then be adjusted to the desired calibration. The linearity of the EODF is 0.25 percent of the full scale. Its resolution is determined by the field of view which can be adjusted by placing spacer rings between the lens and main body of the EODF. The field of view is set for the the displacement range of interest. High resolution requires a small field of view whereas larger fields of view correspondingly reduce the resolution. Table 1 lists various fields of view and their resolutions. The wide range of resolutions makes the EODF a particularly valuable tool for examining sample failure. The resolution used in these tests was about 0.001 mm.

TABLE 1. FIELD OF VIEW AND TYPICAL RESOLUTIONS FOR THE EODF

Field of View	Resolution
10 mm	0.002 mm
5	0.001
1	0.0002

The ram guide ensures that the measured displacement follows the sample displacement as closely as possible, and also serves to keep the applied force in the vertical direction. The ram shaft and guide fit together with close tolerances, so there is little play, but the contact surfaces are highly polished so the ram slides freely in the guide. Both pieces and the guide supports are made of hardened (42 Rockwell) stainless steel and this assembly is bolted to the base of the DWMPT. The guide is bolted to the supports so that samples of various length can be accommodated.

The force transmitted through the ram to the sample is measured by the force transducer mounted on a stainless steel base. The output of the transducer is fed into a Kistler charge amplifier, Model 504E. The gage and amplifier were calibrated as a unit on an Instron, Model TTC, Universal Testing Instrument by applying a known load to the transducer, grounding the amplifier input, quickly releasing the load, and noting the change in the amplifier output voltage. This method eliminates almost all amplifier drift since the output voltage is generated very quickly.

The data acquisition for propellants is performed as illustrated in Figure 4. The outputs of the displacement follower and the charge amplifier are fed into a Nicolet, Series 2090, Explorer III Digital Oscilloscope which records the data on two time-based channels. These data are stored on a floppy disk and later analyzed on a PDP 11/45 computer. A second method is illustrated in Figure 5 and was used in the calibration of the DWMPT. The data are fed directly into the computer through the four channels needed during the calibration procedure.

#### B. The Procedure

For the calibration of the DWMPT, right circular cylinders with a length of 11.4 mm, a diameter of 6.36 mm, and made of 7075-T6 aluminum were used. The dimensions approximate propellant grain size and the material was chosen because it has a strain rate independent elastic modulus at the rates tested,<sup>10</sup> providing a standard for high strain rate testing. The aluminum cylinders were placed in the drop weight tester as described in the Introduction. Two Micro-Measurements precision strain gages, Model EA13-125BT-120, were mounted on opposite sides of the cylinder, as illustrated in

---

<sup>10</sup>T. Nichols, "Dynamic Tensile Testing of Structural Materials Using a Split Hopkinson Bar Apparatus," Report Number AFWAL-TR-80-4053, p. 22, Materials Laboratory, Air Force Wright Aeronautical Laboratories, Wright Patterson Air Force Base, OH, October 1980.

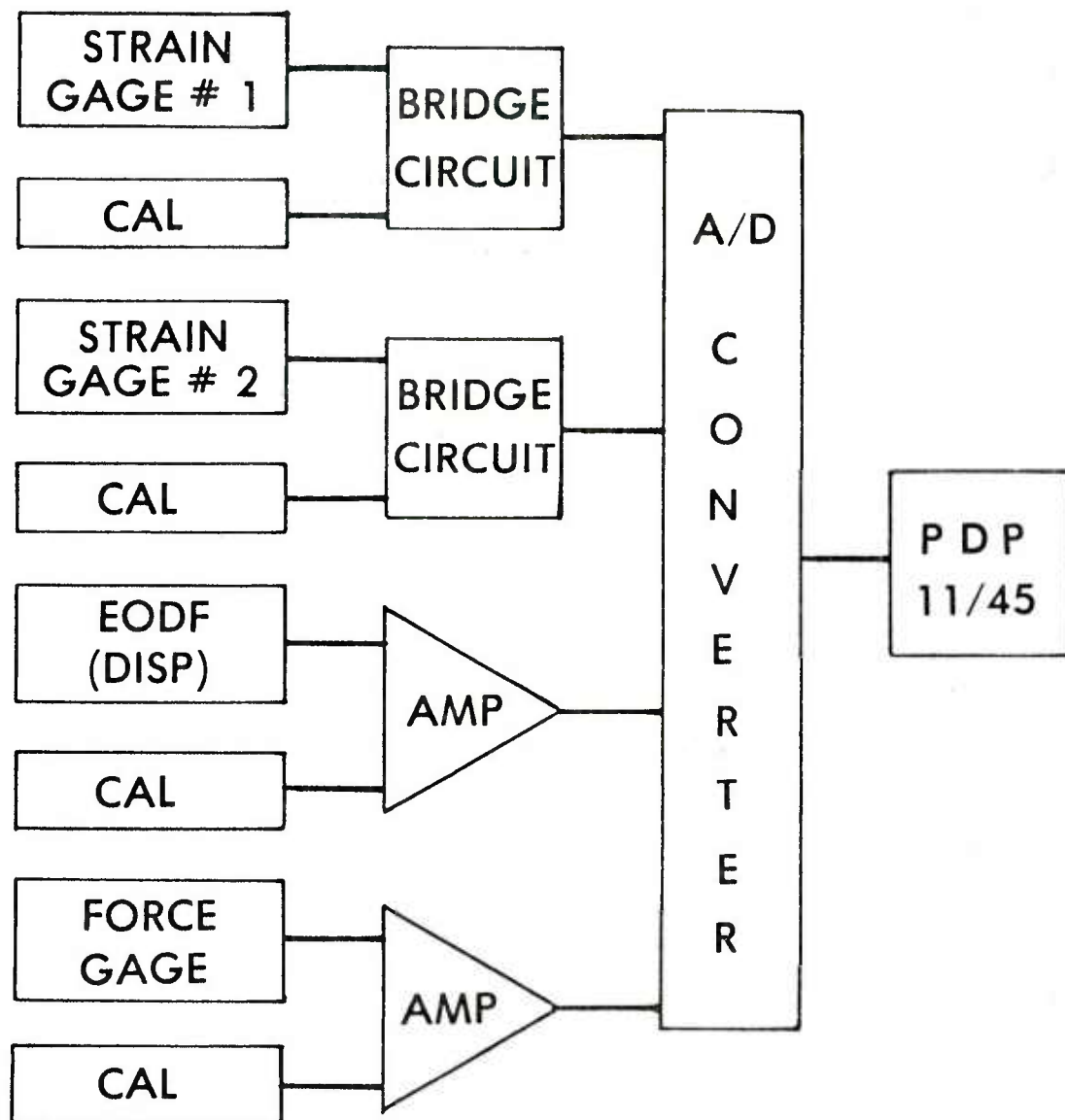


Figure 4. Schematic Diagram of the Data Acquisition During Standardization.

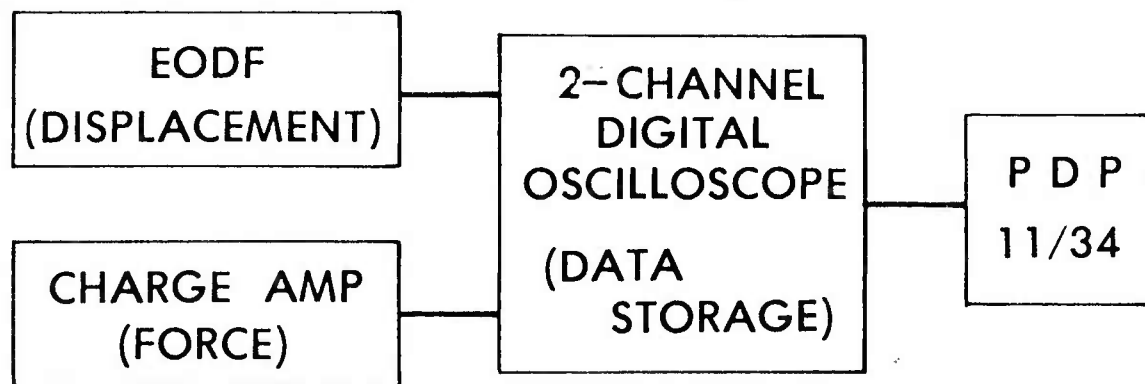


Figure 5. Schematic Diagram of the Data Acquisition During Normal Testing.



Figure 6. These gages provided additional data, as described below. One cylinder was tested with its ends left unlubricated, while the other had a light oil applied to the ends prior to testing.

There are few actual measured values for the compressional modulus, since this measurement is difficult to perform. The sample-mounted strain gages provided independent confirmation of the handbook modulus value, and also monitored any sample bending that may have taken place during compression. The average strain gage value was used for the modulus computation.

During the impact tester standardization, two aspects of the rig were carefully examined. First, the rig motion during the drop test was measured. Compensation for this motion was incorporated into the calculation of the modulus. Then, the degree of sample bending introduced by the rig during testing was also determined. These tests were necessary for the proper interpretation of the data and are described more completely below.

The drop weight for the modulus standardization tests was 1 kg and the drop height, the distance the weight cage falls before impact, was 11 cm. These values provided the proper combination of a moderately high strain rate (between 45 and 50 per second) and significant displacement (about 0.110 mm) without exceeding the range of the force transducer. For the noncoaxial impact (bending) tests the drop height was changed to 5 cm to reduce the possibility of cylinder damage. The drop weight remained at 1 kg.

#### C. The Effect of the Rig Motion on Sample Displacement

The method described above for the optical measurement of displacement can cause the measured values to be larger than the actual sample displacement since the motion of the apparatus itself will be added to any sample compression. This is especially true if the samples have a large modulus. Since the displacement follower is mounted independently of the impact tester, any compression of the ram, or movement of the force transducer, base, or anything below the drop weight tester will be recorded as displacement of the sample. To correct for this, consider the following: If

$E_R$  = Effective Rig Modulus.

$E_C$  = Corrected or True Modulus.

$E_0$  = Optron Measured Modulus.

$F$  = Force Applied to the Sample.

$A$  = Sample Cross Sectional Area.

$dL$  = Total Measured Change in Length.

$L$  = Sample Length.

$dL_s$  = Actual Change in Sample Length.

$dX$  = Displacement Due to Rig Motion.

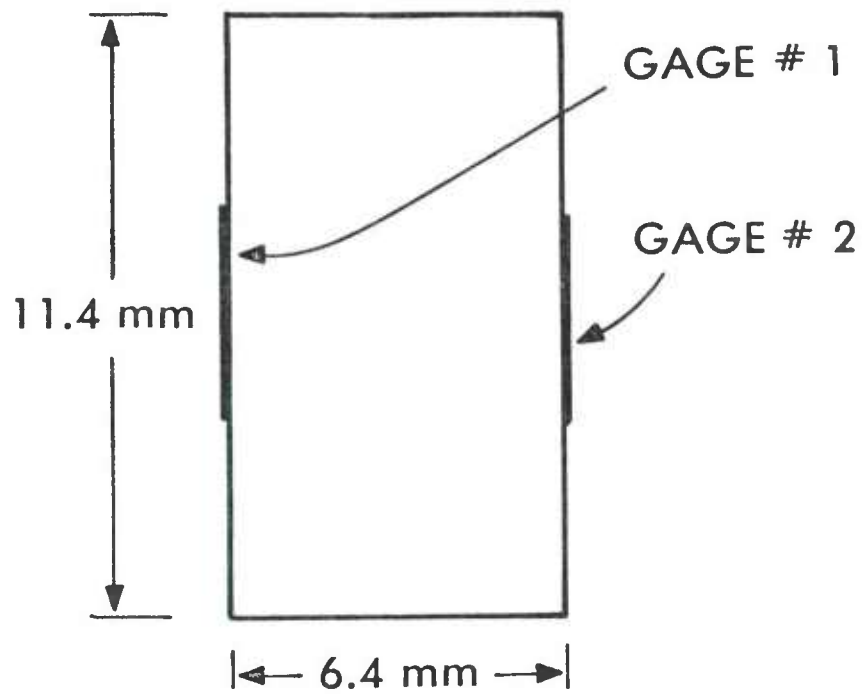


Figure 6. Sample Showing the Location of the Strain Patches.

Then

$$E_0 = \sigma_0 / \epsilon_0, \quad (1)$$

where

$$\sigma_0 = F/A$$

$$\epsilon_0 = dL/L$$

Therefore

$$\begin{aligned} E_0 &= \sigma_0 / (dL/L) \\ &= \sigma_0 / [(dL_s + dX)/L] \\ &= \sigma_0 / [dL_s/L + dX/L] \end{aligned} \quad (2)$$

Or

$$\begin{aligned} 1/E_0 &= (dL_s/L) / \sigma_0 + (dX/L) / \sigma_0 \\ &= 1/E_C + 1/E_R. \end{aligned} \quad (3)$$

Where

$$\begin{aligned} E_R &= \sigma_0 / (dX/L) \\ &= (F/A) (L/dX) \\ &= (F/dX) (L/A) \\ &= S (L/A), \end{aligned} \quad (4)$$

and S is the slope of the force vs displacement curve of the rig (Figure 7). The correct value of the modulus is then given by

$$1/E_C = 1/E_0 - 1/E_R \quad (5)$$

Thus, it can be seen that if  $E_C \ll E_R$ , then  $E_C \approx E_0$ , and no correction is necessary. However, the closer  $E_C$  is to  $E_R$  the lower  $E_0$  will be. As a result, a correction has to be considered for aluminum, which has a relatively high modulus, whereas the propellant modulus may be low enough so that no correction is required.

#### D. The Test for Noncoaxial Impact (Bending)

An aluminum sample was tested with the drop height set at 5 cm and the drop weight set to 1 kg. After testing, the sample was then rotated  $90^\circ$  about the longitudinal axis of the cylinder and tested again. This procedure was repeated and concluded with a final test at the original orientation. The difference in the strain measured by the strain patches mounted on opposite sides of the cylinder is a measure of the bending that the sample has undergone during impact.

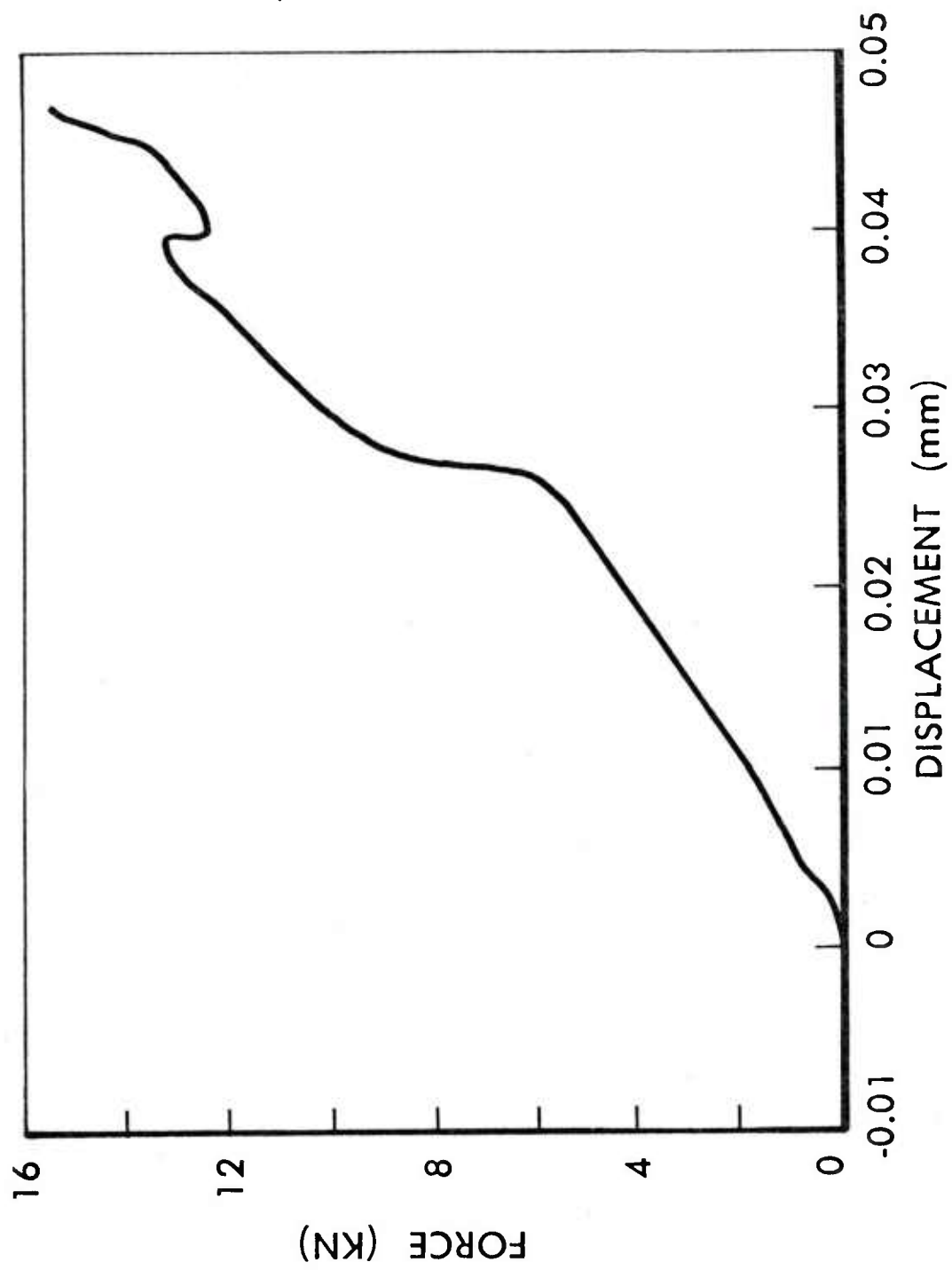


Figure 7. Force Versus Displacement Recorded with No Sample Present in the DWMPT.

If sample bending during compression is due to nonparallel sample faces, then the degree of bending should be independent of the orientation, since the strain gages rotate with the sample. If bending is due to nonparallel rig surfaces or repeated eccentric impacts, then the relative bending should vary sinusoidally with orientation. It is most likely that both causes contribute to bending. If the percent difference in strain,  $Y$ , is plotted against orientation,  $\theta$ , and fitted to Equation 6,

$$Y = A + B \cos (\theta - \theta_0) \quad (6)$$

then  $A$  represents the amount of bending due to the cylinder end surfaces and  $B$  represents the maximum amount due to the rig. Once  $A$  and  $B$  are found then the degree of bending due to the rig can be determined.

### III. RESULTS AND DISCUSSION

#### A. The Rig Motion

Rig motion results in lower modulus values due to the larger optical displacement measurements, discussed earlier. Figure 8 shows the force and displacement vs time curve acquired with no sample in the rig. From these data, the slope of the force vs displacement curve, shown in Figure 7, can be determined. If the slope of this curve is substituted into Equation 4, the "effective rig modulus" for a sample of these dimensions can be determined. An average slope of  $389 \pm 30$  kN/mm was found for the Drop Weight Mechanical Properties Tester.

It should be noted that with no sample in the DWMPT there is a strong tendency for ringing to occur upon impact. This ringing is due to the shock wave generated when the two hard surfaces come into contact, and continues due to reflection at the boundaries of the ram and force transducer. This wave is not noticed with a sample in the impact tester since any shock wave generated is initially much smaller and is attenuated rapidly by the impedance mismatch between the ram, sample, and gage.

#### B. The DWMPT Standardization

Two samples of the 7075-T6 aluminum were used for the standardization of the DWMPT. Sample 1 had its ends unlubricated while Sample 2 had a small amount of light oil added to each end to help keep the faces from binding upon compression. A graphical representation of the data obtained is given in Figures 9 through 13. Figure 9 shows the stress and the EODF strain for a typical event. Figures 10 and 11 indicate the stress and strain region that is used in the calculation of the modulus for the strain gage and EODF measurements, respectively. Figures 12 and 13 show the stress vs strain over the same regions used in Figures 10 and 11, respectively. From these curves, a least squares fit to a straight line is made to determine the modulus of the aluminum. Table 2 lists the results, with no correction for rig motion, for these two samples.

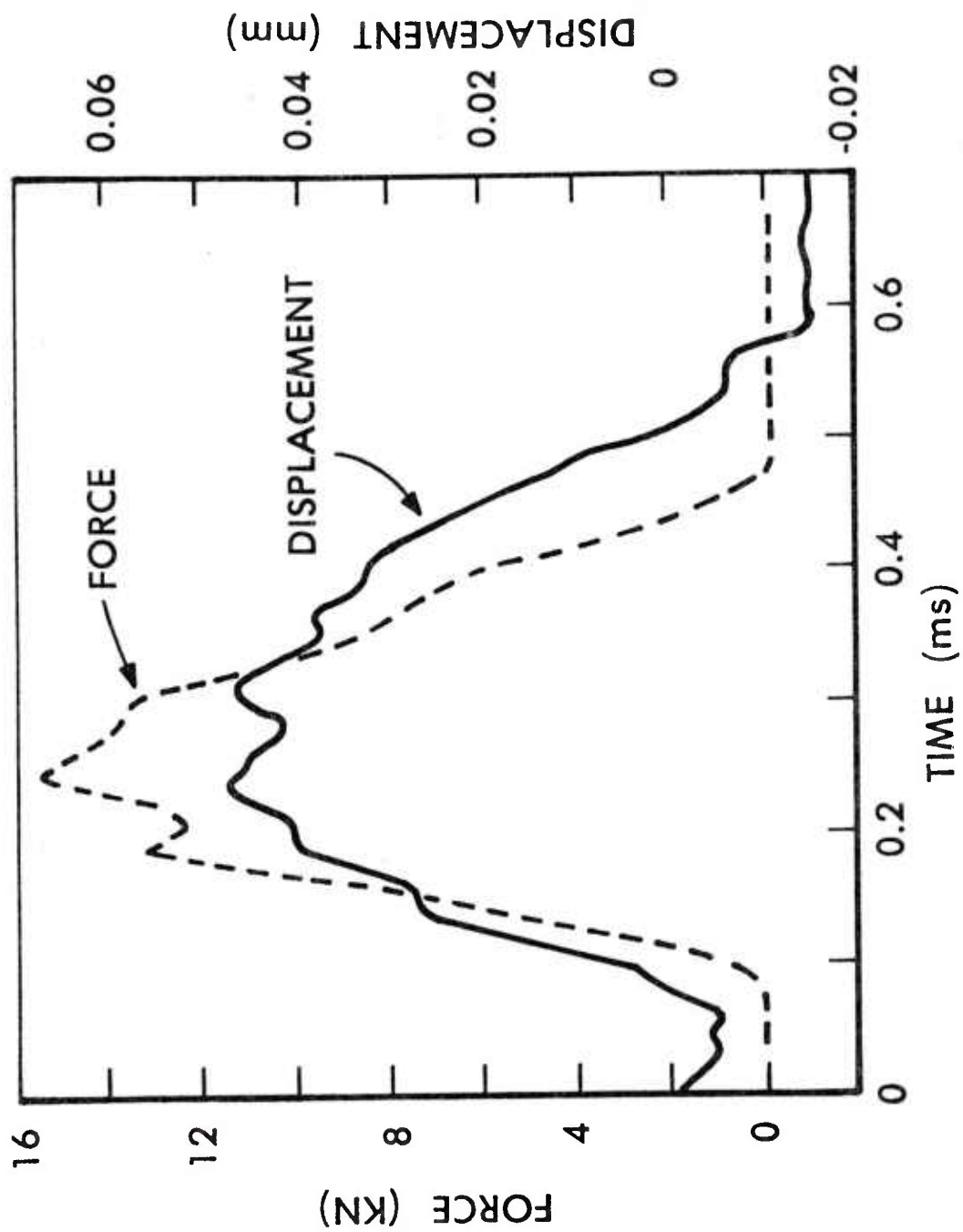


Figure 8. Force and Displacement Versus Time Recorded with No Sample Present in the DMMPT.



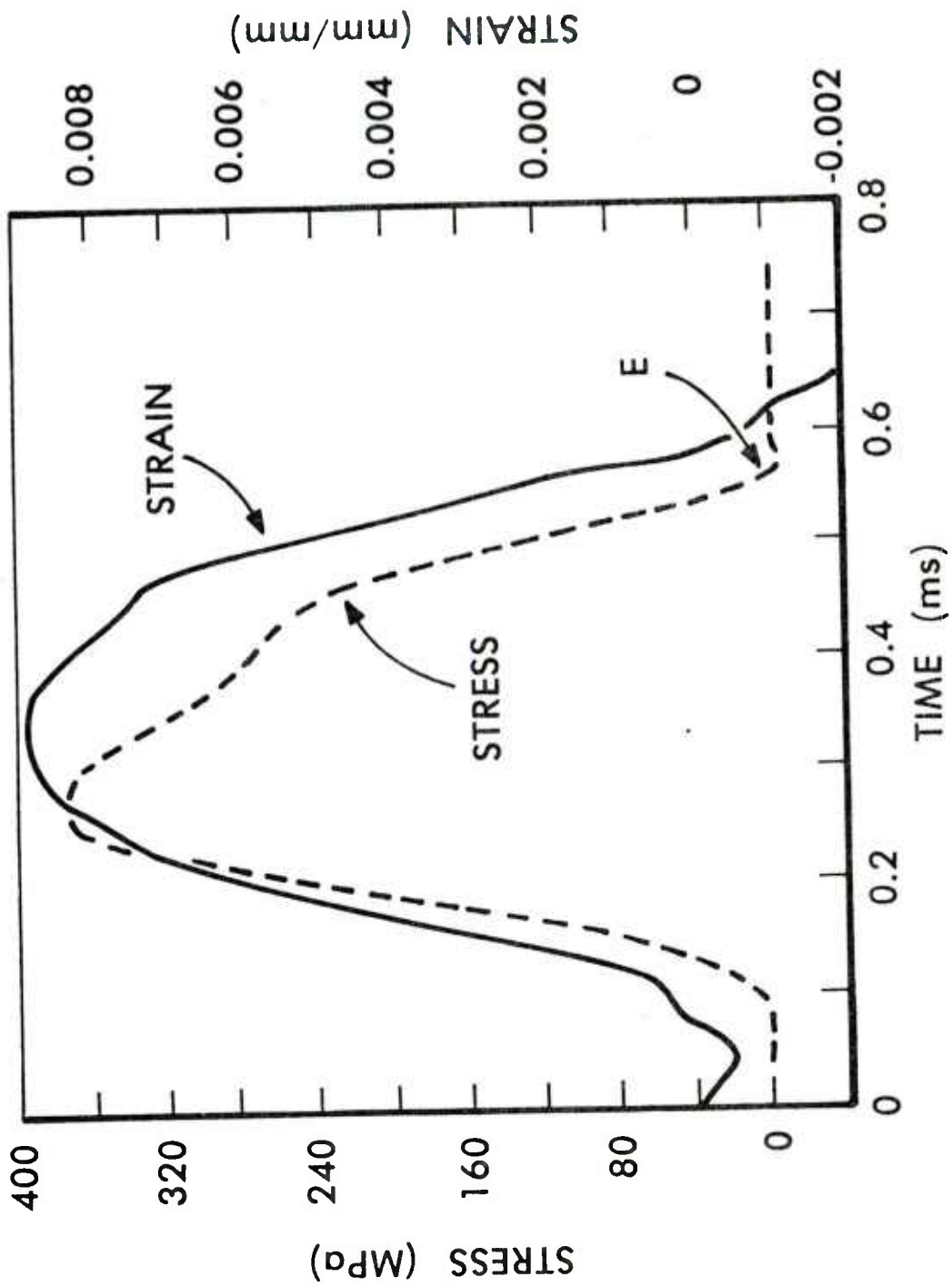


Figure 9. Stress and Strain Versus Time for 7075-T6 Aluminum.

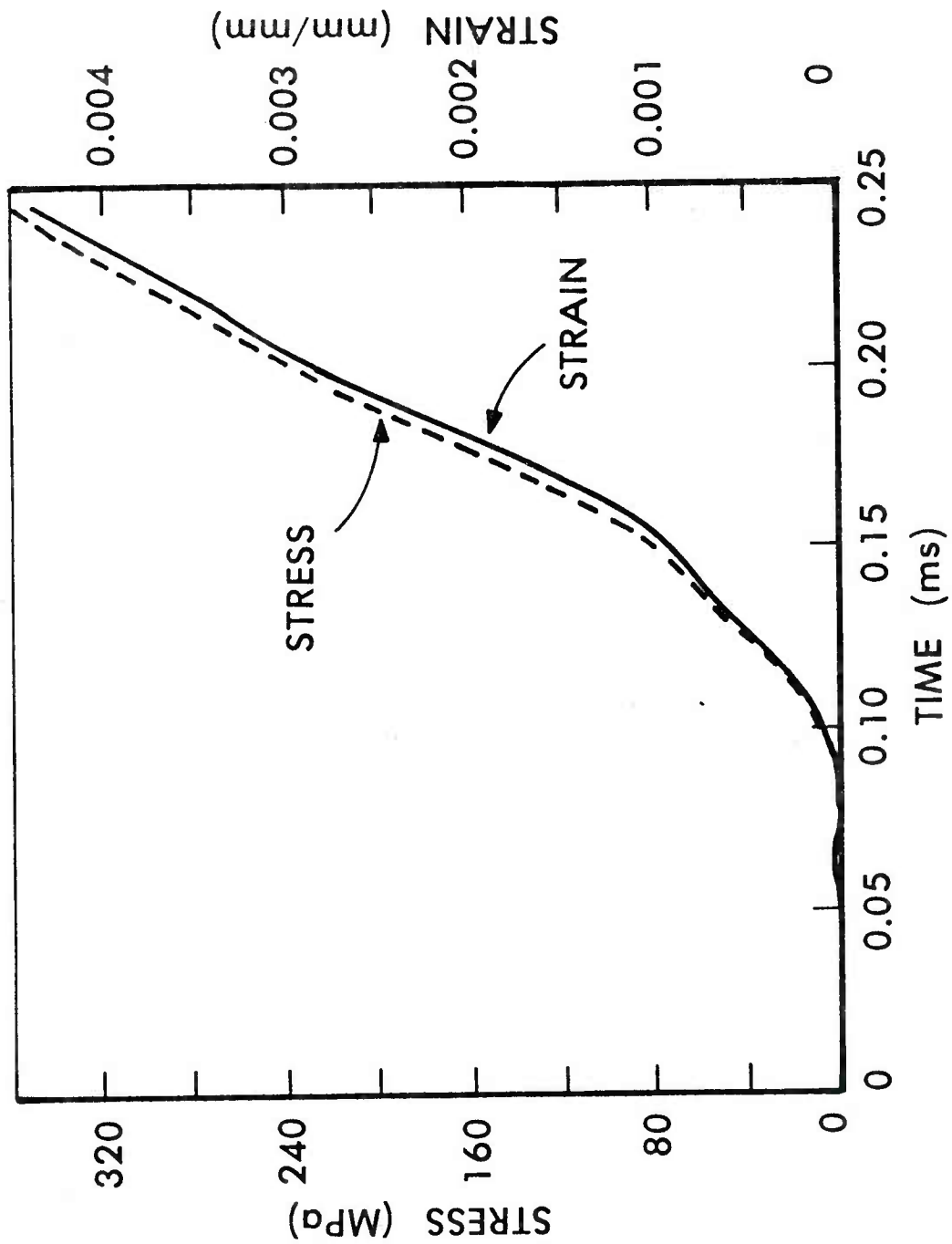


Figure 10. Stress and Strain Versus Time for the Event Shown in Figure 9  
Using the Strain Gage Generated Data.

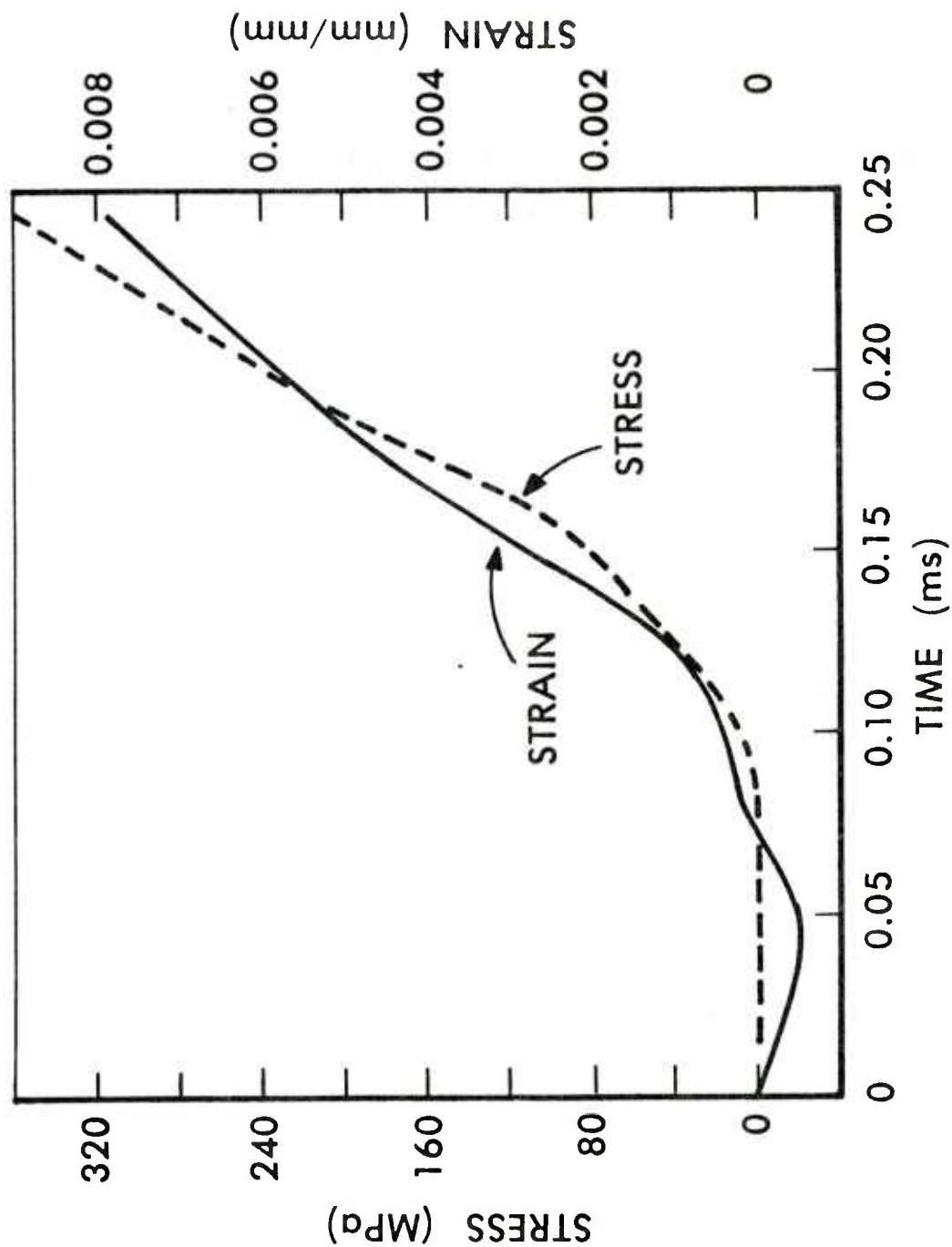


Figure 11. Stress and Strain Versus Time for the Event Shown in Figure 9 Using the Optical Displacement Follower Generated Data.

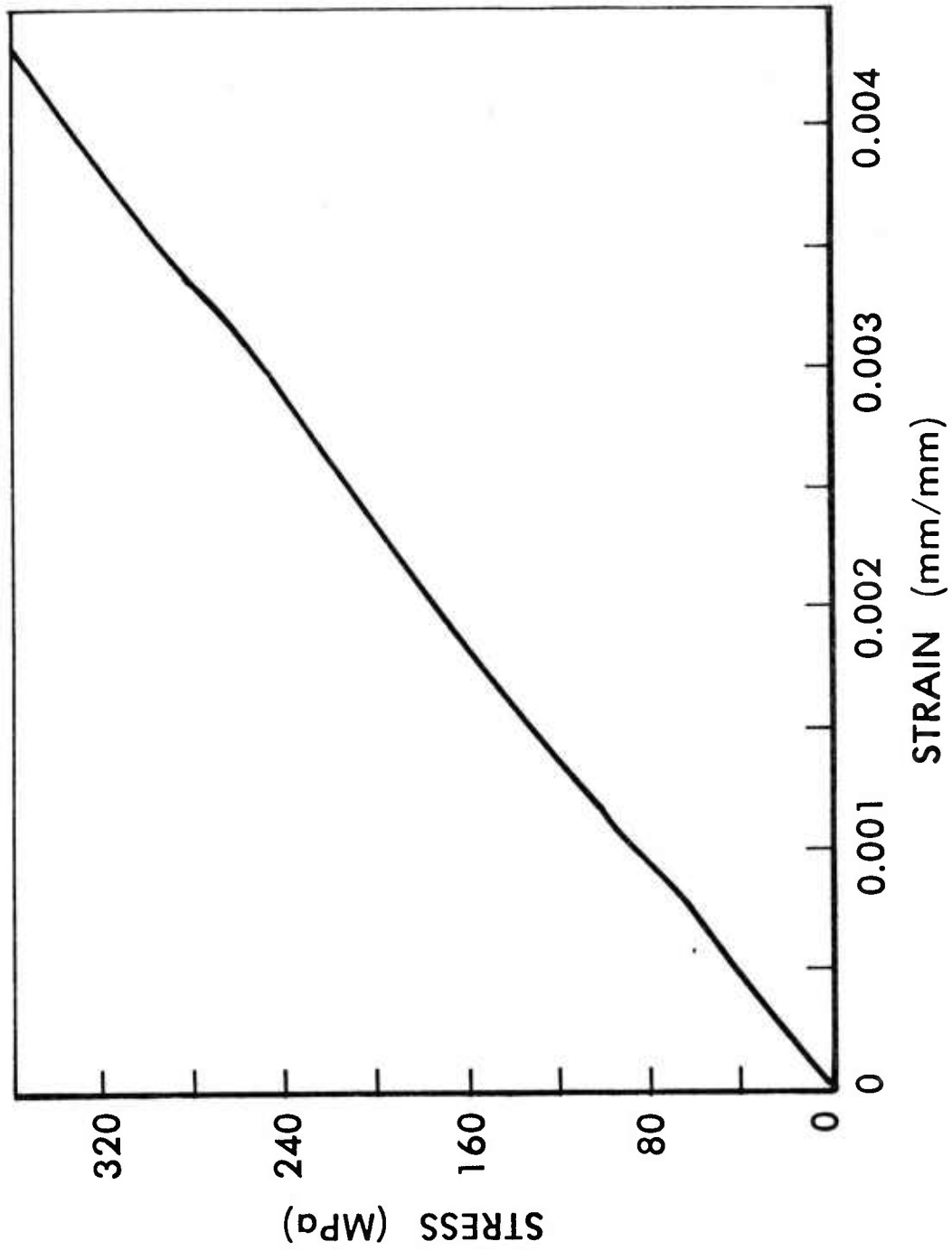


Figure 12. Stress Versus Strain for the Curves Shown in Figure 10

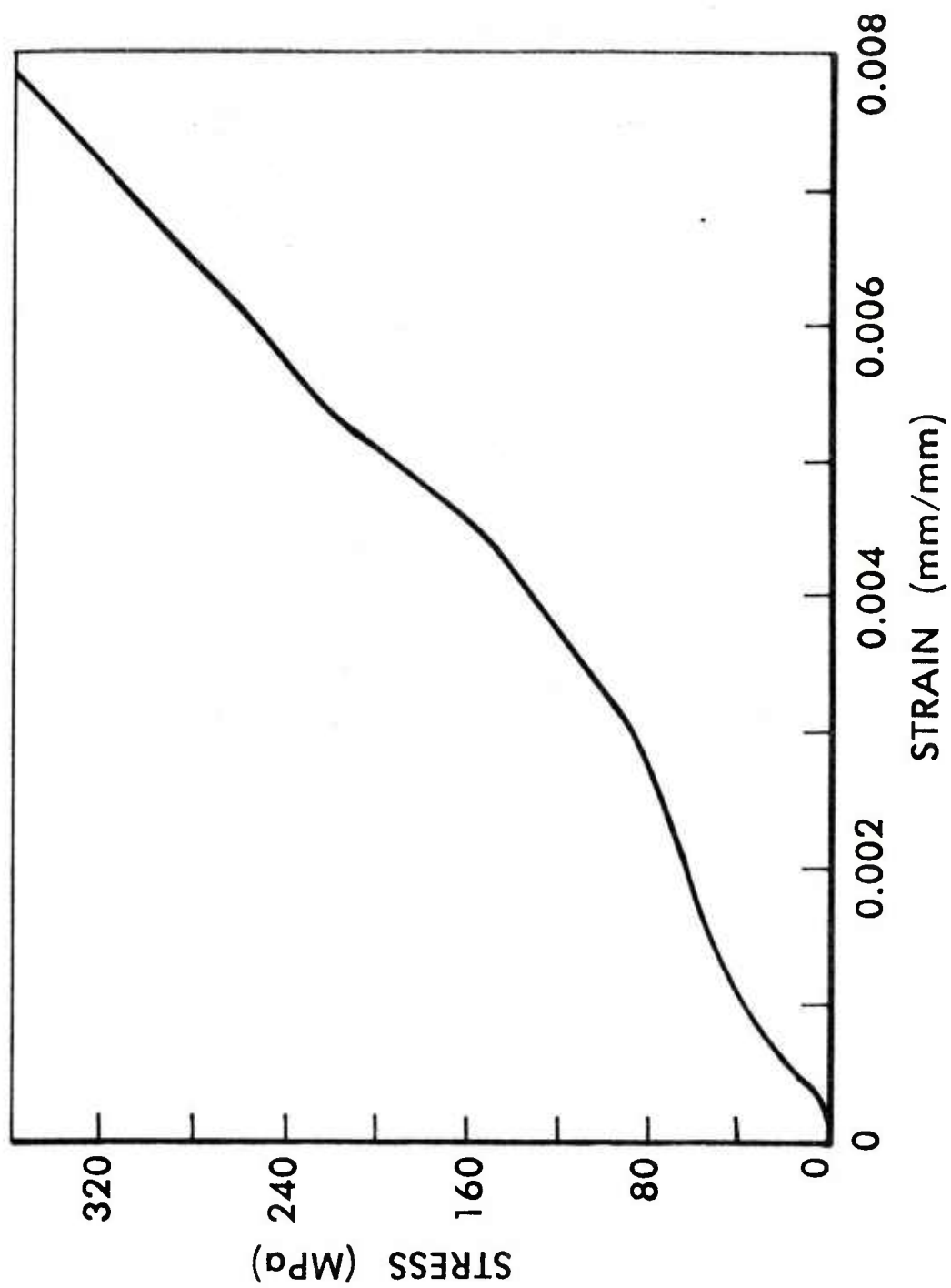


Figure 13. Stress Versus Strain for the Curves Shown in Figure 11

TABLE 2. DROP WEIGHT TEST RESULTS FOR 7075-T6 ALUMINUM  
(Uncorrected for Rig Motion)

Sample 1 - Nonlubricated Ends

Drop	$E_G$	$E_0$
1	80.0 GPa	41.8 GPa
2	79.3	50.6
3	80.3	56.1
4	80.0	50.8
Avg.	$79.9 \pm 0.4$	$52.5 \pm 2.5^*$

Sample 2 - Lubricated Ends

1	80.0	38.1
2	85.0	48.5
3	83.8	47.1
4	82.5	48.9
Avg.	$82.8 \pm 1.8$	$48.2 \pm 0.8^*$

\* Excludes First Drop.

Inspection of these results reveals the following observations. First, all the optical displacement measured modulus values are significantly lower than the gage measured values. This indicates that the rig compliance is significant for these measurements. Next, the  $E_0$  values for the first drops deviate markedly from the values measured on subsequent drops. Also, there is a significant difference in the  $E_0$  values because of the difference in binding between the lubricated and nonlubricated sample ends. This difference is likely to also be responsible for the larger scatter in the nonlubricated  $E_0$  values. Finally, the strain gage measured modulus produces fairly consistent values with  $E_G$  averaging 81.4 GPa, for both the lubricated and unlubricated samples. This is higher than the accepted tensile value of  $E = 71.7$  GPa,<sup>11</sup> but compressional tests usually yield higher modulus measurements.

The overall lower values obtained for EODF measured moduli are due to rig motion. The effective rig modulus calculated from Equation 4 for the aluminum samples is  $E_R = 140 \pm 10$  GPa. (Note,  $E_R$  is dependent on sample dimensions.) This value can now be used in Equation 5 to obtain the corrected modulus value. Table 3 shows these corrected modulus values using this  $E_R$ .

The lower moduli measured on the first drop of the EODF values are the result of small polishing ridges present on the sample ends. Larger

<sup>11</sup> Aluminum Standards and Data 1982, p. 32, The Aluminum Association, Inc., Washington, DC, 1982.



TABLE 3. 7075-T6 ALUMINUM RESULTS AFTER DWMPT CORRECTION

	$E_G$ GPa	$E_0$ GPa	$E_C$ GPa
<u>Nonlubricated Ends</u>	79.9	52.5	84.0
<u>Lubricated Ends</u>	82.8	48.2	73.0

displacements caused by the deformation or flattening of these ridges during the first drop produce an apparently lower modulus as determined with the displacement follower. The strain gage measured values are not sensitive to the displacements produced by end deformation, and do not show this first drop effect.

The higher moduli measured by the strain gages can be understood in terms of the binding that takes place at the upper and lower sample surfaces during compression. Friction between the surfaces of the sample and anvil causes the measured value of the modulus to be higher than the actual value because the limited radial displacement results in limited axial displacement. The degree of binding will determine how much larger the measured modulus will be. With no slippage between the surfaces, the apparent modulus can be shown by calculation to be 1.5 times the tensile value. This effect is demonstrated by comparing the EODF values for the lubricated and unlubricated samples. It is not completely understood why this same trend is not repeated for the strain gage values. However, it is not unreasonable to suspect that strain gages, mounted some distance from the sample ends, would be less sensitive to this effect than the optically measured values due to the difference in the field over which the strain measurement is made. For the strain gages this field is somewhat isolated from the ends, whereas the displacement follower utilizes the entire length of the sample for its strain measurement. This effect is shown in Table 3 by noting the difference between the lubricated and unlubricated values.

By taking the motion of the drop weight tester into account, the apparatus has been shown to give average, high strain rate values for modulus that agree with the strain gage values within 5 percent, and are within 9 percent of the standard handbook value. It should also be pointed out that since the modulus of most propellants is much lower (0.2 to 2.5 GPa) than that of aluminum, larger displacements will be measured for propellant grains. This will reduce the uncertainty in the displacement measurements by increasing the optical displacement follower signal to noise ratio, and result in more accurate modulus measurements.

#### C. The Test for Noncoaxial Impact (Bending)

Figures 14 and 15 show the results from one of the bending tests. Figure 14 shows typical curves comparing the strains on opposite sides of the aluminum cylinder during compression. Figure 15 shows the percent difference in strain during the impact. These values are calculated by taking the difference in strain and dividing by the average strain. The large values at the beginning and end of the event are due to large relative differences at small strains. The average percent difference was calculated using only

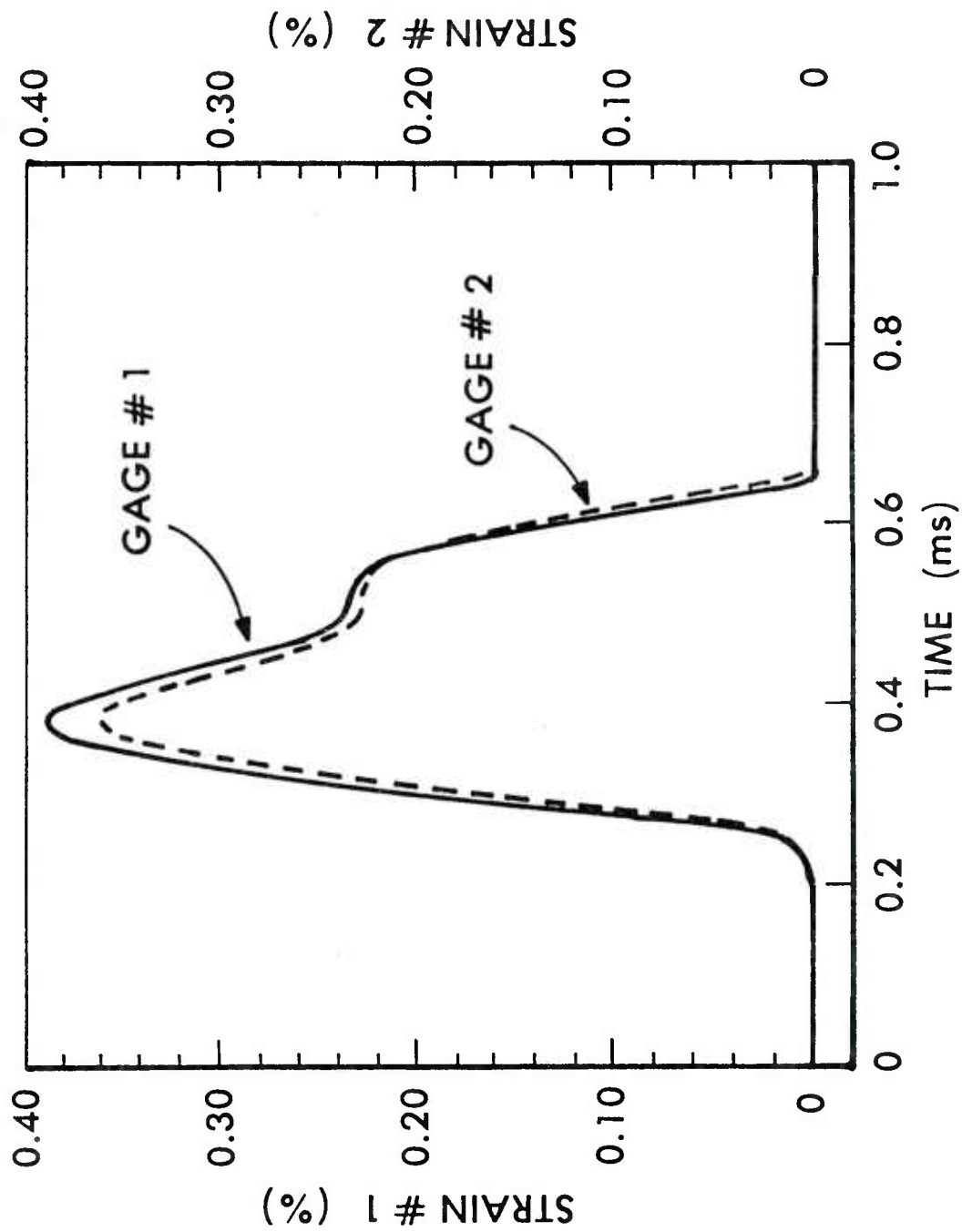


Figure 14. Strain from Strain Gages #1 and #2 Versus Time Recorded During the Bending Test.

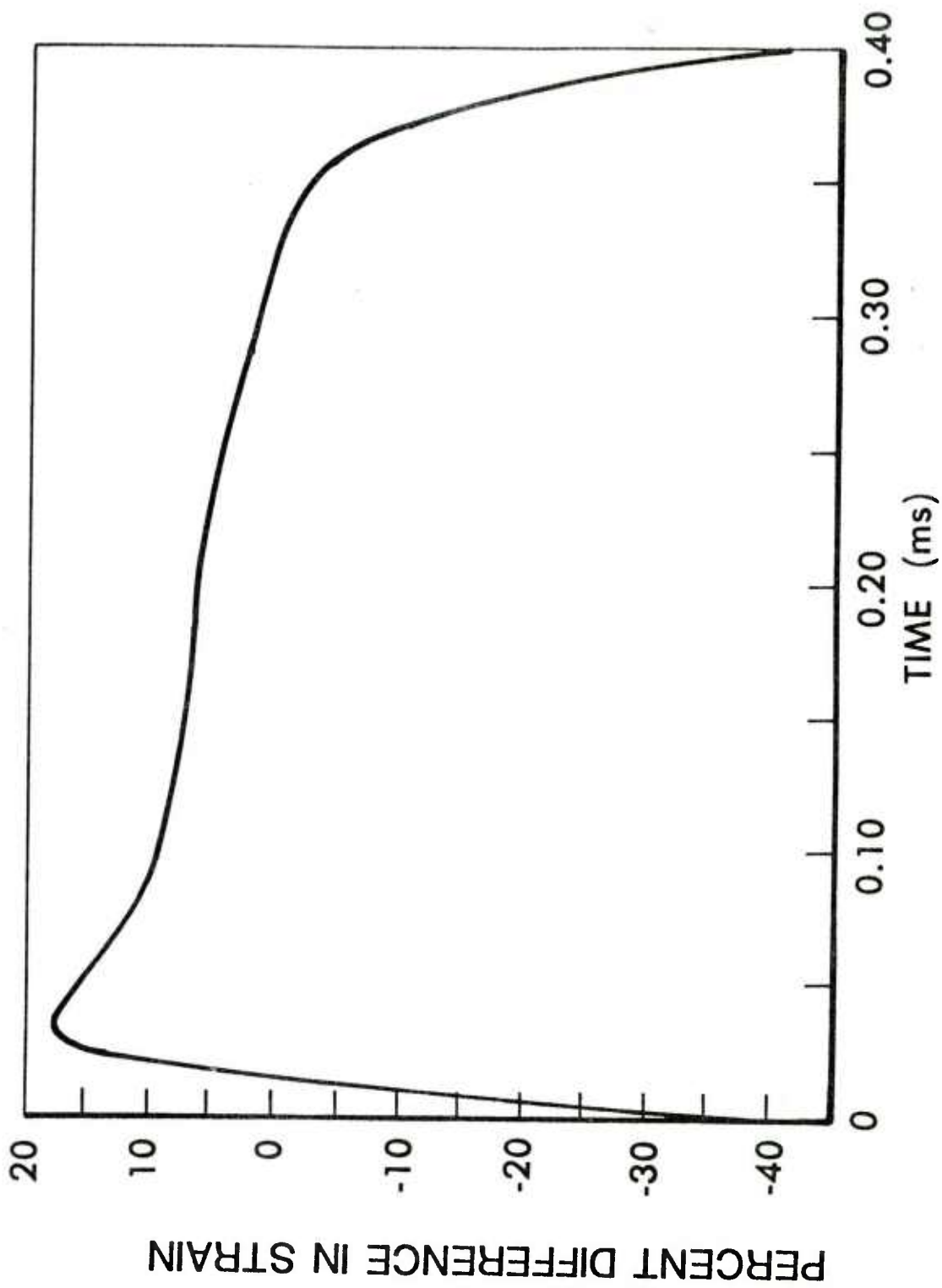


Figure 15. Percent Difference in Strain Recorded from Gages #1 and #2 Versus Time.

strains larger than 25 percent of the maximum strain. These averages for the five drops are listed in Table 4.

TABLE 4. BENDING TEST RESULTS FOR 7075-T6 ALUMINUM

Orientation	Average % Difference in Strain
0 deg	10 %
90	31
180	-18
270	-5
360	7

The data were fit to Equation 6 and the values determined for A and B are  $A = 4.1$  and  $B = 22.4$  with  $\theta_0 = 53.6$  degrees. Figure 16 shows how this curve compared with the data. This indicated that out of a maximum possible 26.5 percent difference in strains, 4.1 percent was due to the sample and 22.4 percent was due to the rig. Since the maximum strain during the bending tests was about 0.5 percent, the maximum difference in strain was 0.13 percent. This value indicated the degree that the compressing surfaces (the ram base and the force gage) were not parallel, and corresponded to a distance, for the 11.4 mm sample, of 0.015 mm. Since the resolution of the EODF was 0.001 mm this effect was measurable, but this difference is much smaller than the expected variations in the distance between the ends of propellant samples. Also, the propellant surface is not expected to be flat to this degree. The rig, therefore, will not cause any bending that may take place during compression of propellant samples.

#### IV. CONCLUSIONS

A technique has been developed to measure the mechanical properties of gun propellant grains at high strain rates. The device measures the sample displacement and impact force simultaneously. It has been standardized with a material that has a strain-rate-independent modulus and was found to give reasonably consistent and accurate results. When testing propellant samples, which generally have moduli an order of magnitude lower than that of aluminum, the accuracy of the results will significantly improve. This is due to the larger displacement measurements and much smaller rig compliance that will be encountered with the softer samples. This development represents significant progress toward the establishment of a simple test to identify propellants with potential performance problems.

#### V. ACKNOWLEDGEMENTS

The authors would like to express their appreciation to the following coworkers who have offered invaluable assistance toward this project. Mr. R. L. Martz and Mr. F. R. Lynn provided guidance and assistance in the data acquisition and reduction. Dr. S. Wise and Dr. B. Burns offered many useful suggestions during the sample testing and data reduction. Also, a special thanks is extended to Mr. A. Koszoru and Ms. M. Hazen for their help in getting the initial measurements under way.

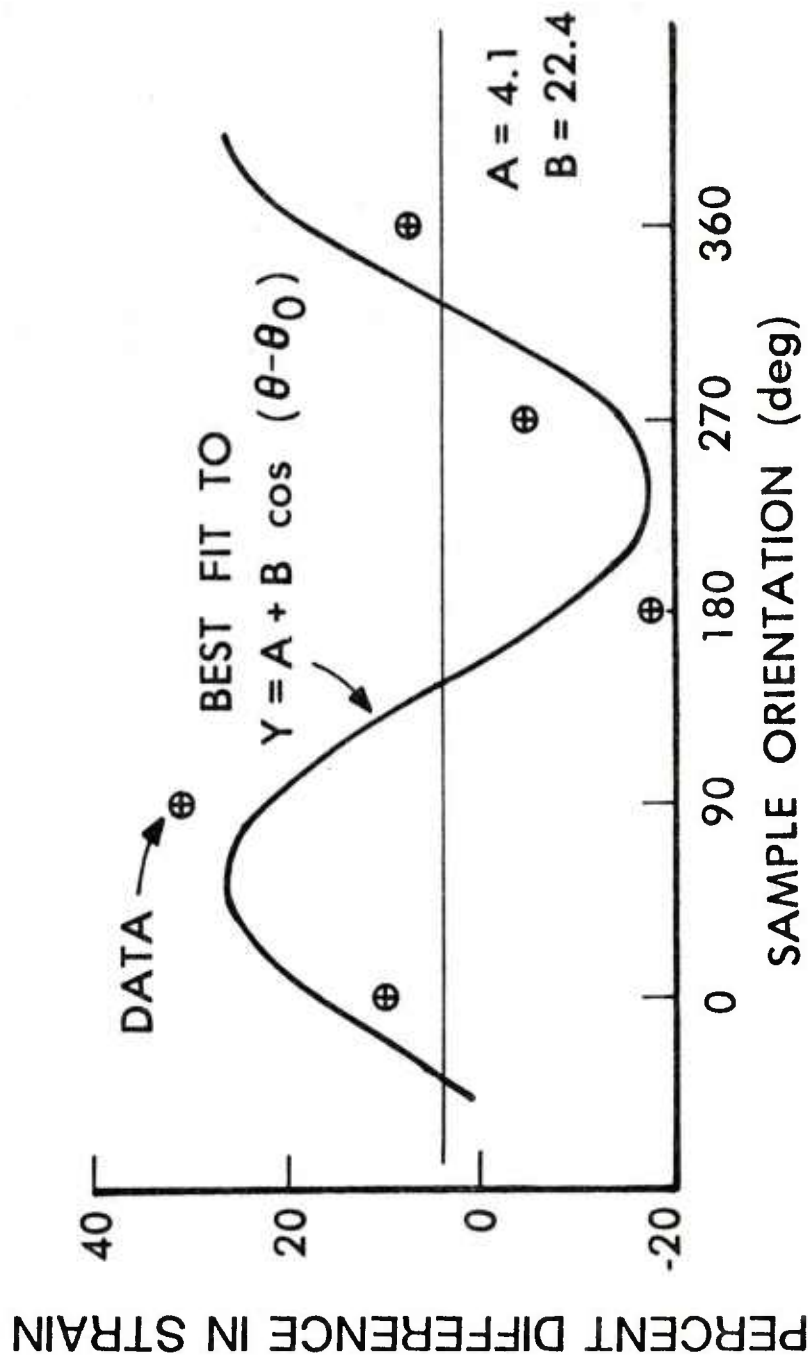


Figure 16. Percent Difference in Strain Versus Sample Orientation Determining the Degree of Bending Due to the DWMPT.

## REFERENCES

1. H. Schubert and D. Schmitt, "Embrittlement of Gun Powder," Proceedings of the International Symposium on Gun Propellants, Dover, NJ, p. 2.11, October 1973.
2. P. J. Greidanus, "Simple Determination of the Mechanical Behavior of Double-Based Rocket Propellants Under High Loading Rates," Propulsion and Energetics Panel, AGARD, 47th (A) Meeting, Paper No. 23, Porz-Wahn, Germany, May 1976.
3. P. Benhaim, J. L. Paulin, B. Zeller, "Investigation on Gun Propellant Break-Up and Its Effect in Interior Ballistics," Proceedings of the 4th International Symposium on Ballistics, Monterey, CA, October 1978.
4. R. A. Wires, J. P. Pfau, J. J. Rocchio, "The Effect of High Rates of Applied Force and Temperature on the Mechanical Properties of Gun Propellants," 1979 JANNAF Propulsion Meeting, Vol. 1, CPIA Publication 300, pp 25-50, March 1979.
5. C. W. Fong, "Mechanical Properties of Gun Propellants - An Assessment of Possible Approaches to Laboratory Testing," Report No. WSRL-0120-TM, Weapons Systems Research Laboratory, Adelaide, South Australia, December 1979.
6. C. W. Fong, "Dynamic Mechanical Properties of Gun Propellants - The Relationship between Impact Fracture Properties and Secondary Loss Transitions," Report No. WSRL-0204-TR, Weapons Systems Research Laboratory, Adelaide, South Australia, March 1981.
7. A. W. Horst, "The Role of Propellant Mechanical Properties in Propelling Charge Phenomenology," 1981 JANNAF Structures and Mechanical Behavior Subcommittee Meeting, Vol. 1, CPIA Publication 351, pp 141-154, December 1981.
8. R. J. Lieb, J. J. Rocchio, and A. A. Koszoru, "Impact Mechanical Properties Tester for Gun Propellants," 1981 JANNAF Structures and Mechanical Behavior Subcommittee Meeting, Vol.1, CPIA Publication 351, pp 155-173, December 1981.
9. C. W. Fong and B. K. Moy, "Ballistic Criteria for Propellant Grain Fracture In the GAU-8/A 30MM Gun, Report not yet published, Direct Fire Weapons Division, Air Force Armament Laboratory, Eglin AFB, FL, December 1981.
10. T. Nichols, "Dynamic Tensile Testing of Structural Materials Using a Split Hopkinson Bar Apparatus," Report Number AFWAL-TR-80-4053, p. 22, Materials Laboratory, Air Force Wright Aeronautical Laboratories, Wright Patterson Air Force Base, OH, October 1980.
11. Aluminum Standards and Data 1982, p. 32, The Aluminum Association, Inc., Washington, DC, 1982.



# DISTRIBUTION LIST

<u>No. Of Copies</u>	<u>Organization</u>	<u>No. Of Copies</u>	<u>Organization</u>
12	Administrator Defense Technical Info Center ATTN: DTIC-DDA Cameron Station Alexandria, VA 22314	3	Commander US Army Materiel Development and Readiness Command ATTN: DRCMD-ST DCRSF-E, Safety Office DRCDE-DW 5001 Eisenhower Avenue Alexandria, VA 22333
1	Office of the Under Secretary of Defense Research & Engineering ATTN: R. Thorkildsen Washington, DC 20301	11	Commander US Army Armament R&D Command ATTN: DRDAR-TD, A. Moss DRDAR-TSS (2 cys) DRDAR-TDC D. Gyorog DRDAR-LCA J. Lannon A. Beardell D. Downs S. Einstein L. Schlosberg W. Westley S. Bernstein Dover, NJ 07801
1	HQDA/SAUS-OR, Washington, DC 20301		
1	HQDA/DAMA-ZA Washington, DC 20310		
1	HQDA, DAMA-CSM, Washington, DC 20310		
1	HQDA/SARDA Washington, DC 20310		
1	Commandant US Army War College ATTN: Library-FF229 Carlisle Barracks, PA 17013	9	Commander US Army Armament R&D Command ATTN: DRDAR-SCA, L. Stiefel B. Brodman DRDAR-LCB-I, D. Spring DRDAR-LCE, R. Walker DRDAR-LCU-CT E. Barrieres R. Davitt DRDAR-LCU-CV C. Mandala E. Moore DRDAR-LCM-E S. Kaplowitz Dover, NJ 07801
1	Commander US Army BMD Advanced Tech Cntr P. O. Box 1500 Huntsville, AL 35804		
1	Chairman DOD Explosives Safety Board Room 856-C Hoffman Bldg. 1 2461 Eisenhower Avenue Alexandria, VA 22331		

# DISTRIBUTION LIST

<u>No. Of Copies</u>	<u>Organization</u>	<u>No. Of Copies</u>	<u>Organization</u>
1	Commander US Army Armament R&D Command ATTN: DRDAR-QAR-R, J. Rutkowski Dover, NJ 07801	5	Commander US Army Armament Materiel Readiness Command ATTN: DRSAR-LEP-L DRSAR-LC, L. Ambrosini DRSAR-IRC, G. Cowan DRSAR-LEM, W. Fortune R. Zastrow Rock Island, IL 61299
5	Project Manager Cannon Artillery Weapons System ATTN: DRCPM-CW, F. Menke DRCPM-CWW H. Noble DRCPM-CWS M. Fissette DRCPM-CWA R. DeKleine H. Hassmann Dover, NJ 07801	1	Commander US Army Watervliet Arsenal ATTN: SARWV-RD, R. Thierry Watervliet, NY 12189
1	Project Manager Munitions Production Base Modernization and Expansion ATTN: DRCPM-PMB, A. Siklosi Dover, NJ 07801	1	Director US Army ARRADCOM Benet Weapons Laboratory ATTN: DRDAR-LCB-TL Watervliet, NY 12189
6	Project Manager Tank Main Armament System ATTN: DRCPM-TMA, K. Russell H. Bernstein, A Albright T. Mahler DRCPM-TMA-105 DRCPM-TMA-120 Dover, NJ 07801	1	Commander US Army Aviation Research and Development Command ATTN: DRDAV-E 4300 Goodfellow Blvd. St. Louis, MO 63120
4	Commander US Army Armament R&D Command ATTN: DRDAR-LCW-A M.Salsbury DRDAR-LCS DRDAR-LC, J. Frasier DRDAR-LCE, D. Wiegand Dover, NJ 07801	1	Commander US Army TSARCOM 4300 Goodfellow Blvd. St. Louis, MO 63120
		1	Director US Army Air Mobility Research And Development Laboratory Ames Research Center Moffett Field, CA 94035
		1	Commander US Army Communications Research and Development Command ATTN: DRSEL-ATDD Fort Monmouth, NJ 07703

# DISTRIBUTION LIST

<u>No. Of Copies</u>	<u>Organization</u>	<u>No. Of Copies</u>	<u>Organization</u>
1	Commander US Army Electronics Research and Development Command Technical Support Activity ATTN: DELSD-L Fort Monmouth, NJ 07703	1	Project Manager Fighting Vehicle Systems ATTN: DRCPM-FVS Warren, MI 48090
1	Commander US Army Harry Diamond Lab. ATTN: DELHD-TA-L 2800 Powder Mill Road Adelphi, MD 20783	1	Director US Army TRADOC Systems Analysis Activity ATTN: ATAA-SL White Sands Missile Range NM 88002
2	Commander US Army Missile Command ATTN: DRSMI-R DRSMI-YDL Redstone Arsenal, AL 35898	1	Project Manager M-60 Tank Development ATTN: DRCPM-M60TD Warren, MI 48090
1	Commander US Army Natick Research and Development Command ATTN: DRDNA-DT, D. Sieling Natick, MA 01762	1	Commander US Army Training & Doctrine Command ATTN: ATCD-A/MAJ Williams Fort Monroe, VA 23651
1	Commander US Army Tank Automotive Command ATTN: DRSTA-TSL Warren, MI 48090	2	Commander US Army Materials and Mechanics Research Center ATTN: DRXMR-ATL Tech Library Watertown, MA 02172
1	US Army Tank Automotive Materiel Readiness Command ATTN: DRSTA-CG Warren, MI 48090	1	Commander US Army Research Office ATTN: Tech Library P. O. Box 12211 Research Triangle Park, NC 27709
1	Project Manager Improved TOW Vehicle ATTN: DRCPM-ITV US Army Tank Automotive Command Warren, MI 48090	1	Commander US Army Mobility Equipment Research & Development Command ATTN: DRDME-WC Fort Belvoir, VA 22060
1	Program Manager M1 Abrams Tank System ATTN: DRCPM-GMC-SA Warren, MI 48090	1	Commander US Army Logistics Mgmt Ctr Defense Logistics Studies Fort Lee, VA 23801

# DISTRIBUTION LIST

<u>No. Of</u> <u>Copies</u>	<u>Organization</u>	<u>No. Of</u> <u>Copies</u>	<u>Organization</u>
2	Commandant US Army Infantry School ATTN: ATSH-CD-CSO-OR Fort Benning, GA 31905	3	Commandant US Army Armor School ATTN: ATZK-CD-MS M. Falkovitch Armor Agency Fort Knox, KY 40121
1	US Army Armor & Engineer Board ATTN: STEBB-AD-S Fort Knox, KY 40121	1	Chief of Naval Materiel Department of the Navy ATTN: J. Amlie Washington, DC 20360
1	Commandant US Army Aviation School ATTN: Aviation Agency Fort Rucker, AL 36360	1	Office of Naval Research ATTN: Code 473, R. S. Miller 800 N. Quincy Street Arlington, VA 22217
1	Commandant Command and General Staff College Fort Leavenworth, KS 66027	2	Commander Naval Sea Systems Command ATTN: SEA-62R R. Beauregard National Center, Bldg. 2 Room 6E08 Washington, DC 20360
1	Commandant US Army Special Warfare School ATTN: Rev & Tng Lit Div Fort Bragg, NC 28307	1	Commander Naval Air Systems Command ATTN: NAIR-954-Tech Lib Washington, DC 20360
1	Commandant US Army Engineer School ATTN: ATSE-CD Ft. Belvoir, VA 22060	1	Strategic Systems Project Office Dept. of the Navy Room 901 ATTN: J. F. Kincaid Washington, DC 20376
1	Commander US Army Foreign Science & Technology Center ATTN: DRXST-MC-3 220 Seventh Street, NE Charlottesville, VA 22901	1	Assistant Secretary of the Navy (R, E, and S) ATTN: R. Reichenbach Room 5E787 Pentagon Bldg. Washington, DC 20350
1	President US Army Artillery Board Ft. Sill, OK 73504	1	Naval Research Lab Tech Library Washington, DC 20375
1	Commandant US Army Field Artillery School ATTN: ATSF-CO-MW, B. Willis Ft. Sill, OK 73503		

# DISTRIBUTION LIST

<u>No. Of</u> <u>Copies</u>	<u>Organization</u>	<u>No. Of</u> <u>Copies</u>	<u>Organization</u>
5	Commander Naval Surface Weapons Center ATTN: Code G33, J. L. East W. Burrell J. Johndrow Code G23, D. McClure Code DX-21 Tech Lib Dahlgren, VA 22448	7	Commander Naval Ordnance Station ATTN: P. L. Stang J. Birkett S. Mitchell L. Torreyson C. Irish D. Brooks Tech Library Indian Head, MD 20640
2	Commander US Naval Surface Weapons Center ATTN: J. P. Consaga C. Gotzmer Indian Head, MD 20640	1	AFSC/SDOA Andrews AFB Washington, DC 20334
4	Commander Naval Surface Weapons Center ATTN: S. Jacobs/Code 240 Code 730 K. Kim/Code R-13 R. Bernecker Silver Spring, MD 20910	1	Program Manager AFOSR Directorate of Aerospace Sciences ATTN: L. H. Caveny Bolling AFB, DC 20332
2	Commanding Officer Naval Underwater Systems Center Energy Conversion Dept. ATTN: CODE 5B331, R. S. Lazar Tech Lib Newport, RI 02840	6	AFRPL (DYSC) ATTN: D. George J. N. Levine B. Goshgarian D. Thrasher N. Vander Hyde Tech Library Edwards AFB, CA 93523
4	Commander Naval Weapons Center ATTN: Code 388, R. L. Derr C. F. Price T. Boggs Info. Sci. Div. China Lake, CA 93555	1	AFFTC ATTN: SSD-Tech Lib Edwards AFB, CA 93523
2	Superintendent Naval Postgraduate School Dept. of Mechanical Engineering ATTN: A. E. Fuhs Code 1424 Library Monterey, CA 93940	1	AFATL/DLYV Eglin AFB, FL 32542
		1	AFATL/DLJM ATTN: W. Dittrich Eglin AFB, FL 32542
		2	AFATA/DLD ATTN: M. Clements J. Schoeneman Eglin AFB, FL 32542
		1	AFWL/SUL Kirtland AFB, NM 87117

# DISTRIBUTION LIST

<u>No. Of Copies</u>	<u>Organization</u>	<u>No. Of Copies</u>	<u>Organization</u>
1	AFATL/DLDL ATTN: O. K. Heiney Eglin AFB, FL 32542	1	Foster Miller Associates ATTN: A. Erickson 135 Second Avenue Waltham, MA 02154
1	AFATL ATTN: DLODL Eglin AFB, FL 32542	2	Calspan Corporation ATTN: Tech Library P.O. Box 400 Buffalo, NY 14225
1	AFFDL ATTN: TST-Lib Wright-Patterson AFB, OH 45433	1	General Applied Sciences Lab ATTN: J. Erdos Merrick & Stewart Avenues Westbury Long Island, NY 11590
1	NASA HQ 600 Independence Avenue, SW ATTN: Code JM6, Tech Lib. Washington, DC 20546	1	General Electric Company Armament Systems Dept. ATTN: M. J. Bulman, Room 1311 Lakeside Avenue Burlington, VT 05412
1	NASA/Lyndon B. Johnson Space Center ATTN: NHS-22, Library Section Houston, TX 77058	1	Hercules, Inc. Allegheny Ballistics Laboratory ATTN: R. B. Miller P. O. Box 210 Cumberland, MD 21501
1	Aerodyne Research, Inc. Bedford Research Park ATTN: V. Yousefian Bedford, MA 01730	1	Hercules, Inc Bacchus Works ATTN: K. P. McCarty P. O. Box 98 Magna, UT 84044
1	Aerojet Solid Propulsion Co. ATTN: P. Micheli Sacramento, CA 95813	1	Hercules, Inc. Eglin Operations AFATL DLDL ATTN: R. L. Simmons Eglin AFB, FL 32542
1	Atlantic Research Corporation ATTN: M. K. King 5390 Cherokee Avenue Alexandria, VA 22314	1	IITRI ATTN: M. J. Klein 10 W. 35th Street Chicago, IL 60616
1	AVCO Everett Rsch Lab ATTN: D. Stickler 2385 Revere Beach Parkway Everett, MA 02149		
2	Calspan Corporation ATTN: Tech Library P. O. Box 400 Buffalo, NY 14225		



# DISTRIBUTION LIST

<u>No. Of Copies</u>	<u>Organization</u>	<u>No. Of Copies</u>	<u>Organization</u>
3	Lawrence Livermore Laboratory ATTN: M. S. L-355, A. Buckingham M. Finger L-201, M. Costantino P. O. Box 808 Livermore, CA 94550	1	Science Applications, Inc. ATTN: R. B. Edelman 23146 Cumorah Crest Woodland Hills, CA 91364
1	Lockheed Missile & Space Co. ATTN: S. McHugn Palo Alto, CA 94304	1	Scientific Research Assoc., Inc. ATTN: H. McDonald P. O. Box 498 Glastonbury, CT 06033
1	Olin Corporation Badger Army Ammunition Plant ATTN: R. J. Thiede Baraboo, WI 53913	3	Thiokol Corporation Huntsville Division ATTN: D. Flanigan R. Glick Tech Library Huntsville, AL 35807
1	Olin Corporation Smokeless Powder Operations ATTN: R. L. Cook P. O. Box 222 St. Marks, FL 32355	3	Thiokol Corporation Wasatch Division ATTN: J. Peterson J. Manser Tech Library P. O. Box 524 Brigham City, UT 84302
1	Paul Gough Associates, Inc. ATTN: P. S. Gough 1048 South Street Portsmouth, NH 03801	2	Thiokol Corporation Elkton Division ATTN: R. Biddle Tech Lib. P. O. Box 241 Elkton, MD 21921
1	Physics International 2700 Merced Street San Leandro, CA 94577	2	United Technologies Chemical Systems Division ATTN: R. Brown Tech Library P. O. Box 358 Sunnyvale, CA 94086
1	Princeton Combustion Research Lab., Inc. ATTN: M. Summerfield 1041 US Highway One North Princeton, NJ 08540	1	Universal Propulsion Company ATTN: H. J. McSpadden Black Canyon Stage 1 Box 1140 Phoenix, AZ 85029
2	Rockwell International Rocketdyne Division ATTN: BA08 J. E. Flanagan J. Grey 6633 Canoga Avenue Canoga Park, CA 91304		



# DISTRIBUTION LIST

<u>No. Of Copies</u>	<u>Organization</u>	<u>No. Of Copies</u>	<u>Organization</u>
1	Veritay Technology, Inc. ATTN: E. B. Fisher P. O. Box 22 Bowmansville, NY 14026	1	University of Minnesota Dept. of Mechanical Engineering ATTN: E. Fletcher Minneapolis, MN 55455
1	Southwest Research Institute ATTN: Robert E. White 8500 Gulebra Road San Antonio, TX 78228	1	Case Western Reserve University Division of Aerospace Sciences ATTN: J. Tien Cleveland, OH 44135
1	Battelle Memorial Institute ATTN: Tech Library 505 King Avenue Columbus, OH 43201	3	Georgia Institute of Tech School of Aerospace Eng. ATTN: B. T. Zinn E. Price W. C. Strahle Atlanta, GA 30332
1	Brigham Young University Dept. of Chemical Engineering ATTN: M. Beckstead Provo, UT 84601	1	Institute of Gas Technology ATTN: D. Gidaspow 3424 S. State Street Chicago, IL 60616
1	California Institute of Tech 204 Karman Lab Main Stop 301-46 ATTN: F. E. C. Culick 1201 E. California Street Pasadena, CA 91125	2	Johns Hopkins University Applied Physics Laboratory Chemical Proplslon Information Agency ATTN: T. Christian H. Hoffmann Johns Hopkins Road Laurel, MD 20707
1	California Institute of Tech Jet Propulsion Laboratory 4800 Oak Grove Drive Pasadena, CA 91103	3	Massachusetts Institute of Technology Dept of Mechanical Engineering ATTN: T. Toong L. Erwin N. Suh Cambridge, MA 02139
1	University of Illinois Dept of Mech Eng ATTN: H. Krier 144 MEB, 1206 W. Green St. Urbana, IL 61801	1	Pennsylvania State University Applied Research Lab ATTN: G. M. Faeth P. O. Box 30 State College, PA 16801
3	University of Massachusetts Dept. of Mechanical Engineering ATTN: K. Jakus J. Chien R. Farris Amherst, MA 01002		

# DISTRIBUTION LIST

<u>No. Of</u> <u>Copies</u>	<u>Organization</u>	<u>No. Of</u> <u>Copies</u>	<u>Organization</u>
1	Pennsylvania State University Dept. Of Mechanical Engineering ATTN: K. Kuo University Park, PA 16802	2	University of Utah Dept. of Chemical Engineering ATTN: A. Baer G. Flandro Salt Lake City, UT 84112
1	Purdue University School of Mechanical Engineering ATTN: J. R. Osborn TSPC Chaffee Hall West Lafayette, IN 47906	1	Washington State University Dept. of Mechanical Engineering ATTN: C. T. Crowe Pullman, WA 99163
1	Rensselaer Polytechnic Inst. Department of Mathematics Troy, NY 12181		<u>Aberdeen Proving Ground</u> Dir, USAMSAA ATTN: DRXSY-D DRXSY-MP, H. Cohen
1	Rutgers University Dept. of Mechanical and Aerospace Engineering ATTN: S. Temkin University Heights Campus New Brunswick, NJ 08903		Cdr, USATECOM ATTN: DRSTE-TO-F STEAP-MT, S. Walton G. Rice D. Lacey C. Herud
1	SRI International Propulsion Sciences Division ATTN: Tech Library 333 Ravenswood Avenue Menlo Park, CA 94025		Dir, HEL ATTN: J. Weisz Dir, USACSL, Bldg E3516, EA ATTN: DRDAR-CLB-PA DRDAR-CLN DRDAR-CLJ-L
1	Stevens Institute of Technology Davidson Laboratory ATTN: R. McAlevy, III Hoboken, NJ 07030		
2	Los Alamos National Lab ATTN: T. D. Butler, MS B216 M. Division, B. Craig P. O. Box 1663 Los Alamos, NM 87545		
1	University of Southern California Mechanical Engineering Dept. ATTN: OHE200, M. Gerstein Los Angeles, CA 90007		

## USER EVALUATION OF REPORT

Please take a few minutes to answer the questions below; tear out this sheet, fold as indicated, staple or tape closed, and place in the mail. Your comments will provide us with information for improving future reports.

1. BRL Report Number \_\_\_\_\_
2. Does this report satisfy a need? (Comment on purpose, related project, or other area of interest for which report will be used.)  
\_\_\_\_\_  
\_\_\_\_\_  
\_\_\_\_\_
3. How, specifically, is the report being used? (Information source, design data or procedure, management procedure, source of ideas, etc.) \_\_\_\_\_  
\_\_\_\_\_  
\_\_\_\_\_
4. Has the information in this report led to any quantitative savings as far as man-hours/contract dollars saved, operating costs avoided, efficiencies achieved, etc.? If so, please elaborate.  
\_\_\_\_\_  
\_\_\_\_\_
5. General Comments (Indicate what you think should be changed to make this report and future reports of this type more responsive to your needs, more usable, improve readability, etc.) \_\_\_\_\_  
\_\_\_\_\_  
\_\_\_\_\_
6. If you would like to be contacted by the personnel who prepared this report to raise specific questions or discuss the topic, please fill in the following information.

Name: \_\_\_\_\_

Telephone Number: \_\_\_\_\_

Organization Address: \_\_\_\_\_  
\_\_\_\_\_  
\_\_\_\_\_